BRL-TR-3360

(2)

TECHNICAL REPORT BRL-TR-3360

BRL

CALCULATION OF ELASTIC-PLASTIC WAVE PROPAGATION ON THE CONNECTION MACHINE

MARK A. OLSON
ARMY HIGH PERFORMANCE COMPUTING RESEARCH CENTER
COMPUTER SCIENCES CORPORATION

KENT D. KIMSEY
U.S. ARMY BALLISTIC RESEARCH LABORATORY

JUNE 1992

U.S. ARMY LABORATORY COMMAND

BALLISTIC RESEARCH LABORATORY
ABERDEEN PROVING GROUND, MARYLAND

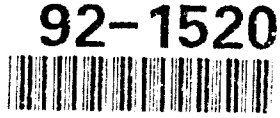

NOTICES

Destroy this report when it is no longer needed. DO NOT return it to the originator.

Additional copies of this report may be obtained from the National Technical Information Service, U.S. Department of Commerce, 5285 Port Royal Road, Springfield, VA 22161.

The findings of this report are not to be construed as an official Department of the Army position, unless so designated by other authorized documents.

The use of trade names or manufacturers' names in this report does not constitute indorsement of any commercial product.

REPORT DOCUMENTATION PAGE

Form Approved
OMB No. 0704-0188

1. AGENCY USE ONLY (Leave blank)	2. REPORT DATE	3. REPORT TYPE AND DATES COVERED
	June 1992	Final, Nov 90–Sep 91

4. TITLE AND SUBTITLE

Calculation of Elastic-Plastic Wave Propagation on the Connection Machine

5. FUNDING NUMBERS

PR: 1L162618AH80

6. AUTHOR(S)

Mark A. Olson[a] and Kent D. Kimsey

7. PERFORMING ORGANIZATION NAME(S) AND ADDRESS(ES)

Army High Performance Computing Research Center
Computer Sciences Corporation
University of Minnesota
1100 Washington Avenue
Minneapolis, MN 55415

8. PERFORMING ORGANIZATION REPORT NUMBER

9. SPONSORING / MONITORING AGENCY NAME(S) AND ADDRESS(ES)

U.S. Army Ballistic Research Laboratory
ATTN: SLCBR-DD-T
Aberdeen Proving Ground, MD 21005-5066

10. SPONSORING / MONITORING AGENCY REPORT NUMBER

BRL-TR-3360

11. SUPPLEMENTARY NOTES

[a]Mark A. Olson is employed by Computer Sciences Corporation, Minneapolis, MN 55415. Performed under the auspices of Army High Performance Computing Research Center, Computer Sciences Corporation, under contract #DAAL03-89-C0088.

12a. DISTRIBUTION / AVAILABILITY STATEMENT

Approved for public release; distribution is unlimited.

12b. DISTRIBUTION CODE

13. ABSTRACT *(Maximum 200 words)*

This report describes the parallel algorithms and data structures for implementing a 2-D multimaterial kernel of the wave-propagation code, HULL, on a Connection Machine. Computational performance is illustrated for a rod-plate impact problem with material strength described through an elastic-perfectly plastic formulation. The hydrodynamic behavior of materials is modeled via the gamma law and Mie-Gruneisen equations of state.

14. SUBJECT TERMS

massively parallel, wave propagation, high performance computing, hypercube, impact

15. NUMBER OF PAGES

25

16. PRICE CODE

17. SECURITY CLASSIFICATION OF REPORT	18. SECURITY CLASSIFICATION OF THIS PAGE	19. SECURITY CLASSIFICATION OF ABSTRACT	20. LIMITATION OF ABSTRACT
UNCLASSIFIED	UNCLASSIFIED	UNCLASSIFIED	UL

INTENTIONALLY LEFT BLANK.

TABLE OF CONTENTS

INTENTIONALLY LEFT BLANK.

LIST OF FIGURES

INTENTIONALLY LEFT BLANK.

ACKNOWLEDGMENT

The computations reported here were made possible by the University of Minnesota AHPCRC Supercomputer Resources.

INTENTIONALLY LEFT BLANK.

1. INTRODUCTION

The emergence of massively parallel computers, such as the present generation of hypercube machines, is having a significant influence on the development and implementation of computational models for describing physical phenomena. A pressing concern in the construction of parallel applications is the mapping of algorithms onto scalable multiprocessors which can be scaled to the teraflop (10^{12} floating point operations per second) performance range.

An important class of problems where the principal limitation is CPU performance is the large-scale numerical solution of partial differential equations applied to shock physics modeling in two and three dimensions. The successful utilization of parallel computers for these problems requires the adaptation of existing sequential algorithms into reliable and robust parallel algorithms.

This report presents a brief overview of the parallel algorithms and data structures for implementing a two-dimensional (2-D), multimaterial kernel of the wave-propagation code, HULL, on a Connection Machine (CM). Computational performance is illustrated for a prototypical rod-plate impact problem. Particular detail is given to computational methodology, performance characteristics, and algorithm scalability. Complementary parallel computing efforts for recently developed wave-propagation codes are being conducted by Sandia National Laboratories (Robinson et al. 1990) and Los Alamos National Laboratory (Hopson 1990).

2. THE CONNECTION MACHINE

The Connection Machine CM-2 (Thinking Machines Corporation 1990) is a massively data-parallel computer configured with a maximum of 64K (2^{16}) bit-serial processors interconnected in a boolean hypercube topology. Each processor is equipped with 128 Kbytes of memory giving a total memory capacity of 8 Gbytes. The processors are arranged in hardware with 16 processors to a chip, and each pair of chips (referred to as a node) share a Weitek floating-point accelerator each having 64-bit precision arithmetic.

Floating point computations on the CM-2 are implemented via two models: fieldwise and slicewise. In the fieldwise model, the atomic unit is the processing element and the storage of a 32-bit word is allocated in 32 sequential bits of a physical processor's memory. In the slicewise model, the atomic unit is the processing node and a word is stored in a 32-bit slice across the memories of the 32 processors in a node. The advantage of the slicewise model is the enhanced efficiency in utilizing the floating-point units derived from converting memory-to-memory operations in the fieldwise model to register-to-register operations in the slicewise.

The granularity of the CM-2 is reflected in the application of virtual sets. For the fieldwise model, this refers to the formation of virtual processors (VPs) and, for the slicewise model, the abstraction of virtual grids. A VP is the segmentation of the local memory of each processor, thus enabling the CM-2 to simulate a system with more physical processors. A virtual grid, in contrast to VPs, does not exist as a formal object in CM memory, but provides a useful way for describing the allocated memory across processing nodes. The run-time system determines allocated memory within the processing elements and maps declared array dimensions onto the virtual grids. The execution of instructions by the virtual sets is performed by time-slicing the physical processing units.

The CM-2 processing units operate in a Single-Instruction Multiple-Data (SIMD) mode, meaning all processors receive the same instruction stream on each cycle. Conditional operations (i.e., masks) permit any subset of the processors to be deselected such that the instruction will only be performed by those processors in the selected set. The instruction stream is broadcast by sequencers which are controlled by a conventional front-end machine. The front-end machine supports the operating and programming environment. Current languages supported include CM-Fortran, C*, *Lisp, and Paris.

Interprocessor communication is carried out using two mechanisms referred to as the NEWS (North-East-West-South) grid and router. The addressing of a VP is based on a Gray coded grid which provides an n-bit cube address (where $n \leq 16$) for specifying the location of the processor on an n-dimensional hypercube. The NEWS addressing scheme allows processors to pass data according to a structured rectangular grid. The router, on the other hand, is the more general mechanism which allows any VP to communicate with any other VP

on the hypercube. In addition, the router allows the local memories of the processors to be treated as a single, large shared memory. The application of the NEWS grid and router for a given problem depends on the data pattern which may vary as a function of time. NEWS communication is the most efficient. As a result, an explicit finite difference scheme, such as HULL, maps efficiently onto the CM since communications are mostly nearest-neighbor (NEWS).

3. THE HULL EULERIAN HYDROCODE

The HULL code (Matuska and Osborne 1987) is a multidimensional, multimaterial Eulerian wave-propagation code that numerically solves the partial differential equations of continuum mechanics. Explicit terms for heat conduction and viscous effects are not included. The equations solved in axisymmetric cylindrical coordinates for 2-D are:

$$\dot{\rho} + \rho\left[\frac{\partial(xu)}{\partial x} + \frac{\partial v}{\partial y}\right] = 0\,, \tag{1.1}$$

$$\rho\dot{u} - \frac{\partial T_{xx}}{x\partial x} - \frac{\partial T_{xy}}{\partial y} + \frac{T_{\theta\theta}}{x} = 0\,, \tag{1.2}$$

$$\rho\dot{v} - \frac{\partial T_{xy}}{x\partial x} - \frac{\partial T_{yy}}{\partial y} = -\rho g\,, \tag{1.3}$$

$$\rho\dot{E} - \frac{\partial}{x\partial x}[x(uT_{xx} + vT_{xy})] - \frac{\partial}{\partial y}(uT_{xy} + vT_{yy}) = -\rho vg\,, \tag{1.4}$$

where ρ is the material density, x and y are the radial and axial coordinates, respectively, u and v are the corresponding radial and axial velocity components, T is the stress tensor, E is the total specific energy, and g is the gravitational body force.

Equations 1.1 through 1.4 are solved on a finite-difference, rectangular mesh composed of discrete spatial intervals, $\Delta x_i, \Delta y_j$, in the radial and axial coordinates. The solution is advanced explicitly from the initial conditions by discrete time steps, Δt^n, and is defined on the mesh (x_i, y_j, t^n) where each of the state variables $\xi(x, y, t)$ in the solution space is defined by $\xi^n_{i,j} = \xi(x_i, y_j, t^n)$.

State variables are defined at the geometric center of each cell. Cell boundary values are interpolated through one computational cycle via cell-centered values from nearest-neighbor cells. These boundary values are then advanced through one-half time step using cell-center to cell-center gradients. This step is then followed by a full-time step using half-time advanced cell-boundary gradients. Lagrangian conservation (Equations 1.1–1.4) is utilized in this time update. To maintain the original Eulerian mesh, material is advected from one cell to another via a first-order donor cell algorithm with a heuristic, multimaterial diffusion limiter to preserve material interfaces.

Material models in HULL include elastic-perfectly plastic with von Mises yield criterion as well as temperature and work hardening effects. The Mie-Gruneisen equation of state (EOS) is used to model solids and liquids, and the gamma law is used to model gases. Explosives are modeled via the Jones-Wilkins-Lee EOS. Material failure models include maximum principal stress, maximum principal strain, and the Hancock-Mackenzie triaxial failure model.

4. PARALLEL IMPLEMENTATION OF HULL

Implementation complexity of adapting the HULL code to a parallel platform depends on several factors—namely, the degree of parallelism, granularity and scalability, interprocessor communication, and I/O demands. To achieve high performance, efficient data parallelism must be constructed which maximizes processor load and streamlines interprocessor communication.

4.1 CM-2 Data Structure. The algorithmic framework for mapping the HULL data structure onto the CM-2 architecture lies in the utilization of both the canonical layout of arrays and the use of the compiler array directive LAYOUT (Thinking Machine Corporation 1989).

Hydrodynamic variable arrays for pressure, velocity, stresses, and strains are canonically allocated one element per VP* with each conformable array being placed in the same virtual set. Conformable arrays have the same shape. Array dimensions are defined in 2-D as

* Formally a distinction should be made between fieldwise and slicewise mapping of arrays. For details, see *Thinking Machines Corporation* (1991).

(0:*nx*, 0:*ny*), where *nx* and *ny* are the number of hydrodynamic computational cells in the *x* and *y* spatial directions, respectively. Each array is buffered with fictitious cells (Figure 1) containing the appropriate boundary conditions. Boundary conditions accounted for include both transmissive and reflective.

Fictitious cells are incorporated into the mesh to perform uniform computations on all active cells at all times independent of whether the cells are internal or boundary cells. This approach maximizes processor utilization during a clock cycle for the Lagrangian and advection computations, thereby decreasing the overall computational grind time. The boundary conditions for the top and right are carried out in parallel while the densities of the fictitious cells are being numerically updated.

All grid axes for the hydrodynamic variable arrays are NEWS-ordered (Figure 2). Elemental operations between the arrays in a virtual set require no interprocessor communication and dimensional shifts on cells, as required in finite-difference schemes, are performed with NEWS communication.

The compiler directive LAYOUT allows the programmer to specify the axis ordering and weights of the virtual set in which an array is allocated. An important application of LAYOUT is for arrays with mixed data-parallel (NEWS-ordered) dimensions and serial dimensions. An example is the mass array shown in Figure 3. Elements are given by xm(:SERIAL, :NEWS, :NEWS), where the SERIAL dimensions span the number of materials (denoted by *nm*) and NEWS the mesh space. Computations over the serial dimensions are performed via the front-end computer whereas the data-parallel dimensions are performed on the CM-2. Similar mixed arrays are constructed for material volumes and energies. Each mixed array can be viewed as an indexed collection (i.e., a material slice) of data-parallel arrays.

4.2 Lagrangian Computations. The cornerstone in reprogramming the Lagrangian step for SIMD operations lies in the functionality of the NEWS communication. Finite-difference schemes are implemented via the application of intrinsic shift functions performed on data-parallel arrays.

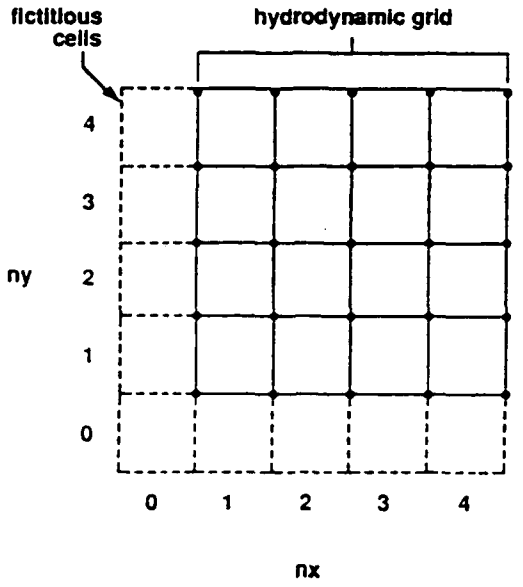

Figure 1. CM-2 Computational Grid.

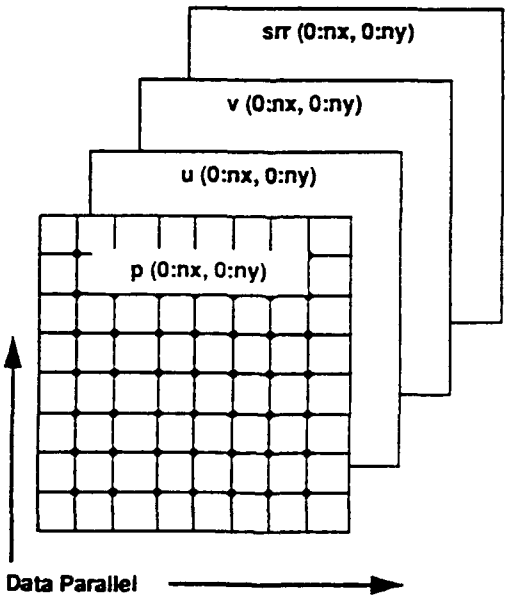

Figure 2. Data-Parallel Hydrodynamic Variable Arrays.

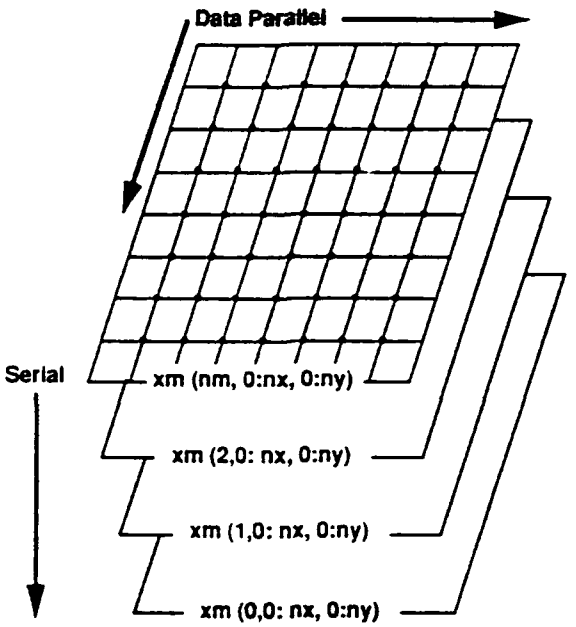

Figure 3. Data-Parallel Material-Indexed Hydrodynamic Variable Arrays.

As an example, the finite-difference representation for the u-component of velocity computed at the cell boundary $i + 1/2$ at time $t = t^n$ is given by:

• Serial Lagrangian

$$u^n_{i+1/2,j} = \frac{\rho^n_{i,j}\, u^n_{i,j} + \rho_{i+1,j}\, u^n_{i+1,j}}{\rho^n_{i,j} + \rho^n_{i+1,j}}; \tag{2}$$

• Data-Parallel Lagrangian

$$u^n_{1/2} = \frac{\rho^n u^n + cshift(\rho^n u^n, 2, 1)}{\rho^n + cshift(\rho^n, 2, 1)}. \tag{3}$$

The key point is the replacement of sequential operations on array elements $\rho^n_{i,j}$, $u^n_{i,j}$ with the global uniform operation on data-parallel arrays ρ^n, u^n. The circular shift, *cshift* (ρ^n,2,1),

has the effect of shifting the data-parallel array ρ^n to the left by one position. This operation is one of the most efficient CM-Fortran operations due to the direct mapping onto the NEWS communication grid. (A caveat is that the grid dimensions must be a power of 2 for fieldwise and multiples of 4 for slicewise.)

The data-parallel solution for the Lagrangian Equations 1.2–1.4 with the assumption $\Delta t = \Delta t^n$ is given by:

$$u^{n+1} = u^n - \frac{\Delta t}{\rho^n}\left[\delta^x \rho^{n+1/2} - \frac{1}{x}\delta^x x S_{xx}^n - \delta^y S_{xy}^n + \frac{S_{xx}^n + S_{yy}^n}{x}\right], \tag{4.1}$$

$$v^{n+1} = v^n - \frac{\Delta t}{\rho^n}\left[\delta^y (S_{yy}^n - P^{n+1/2}) \frac{1}{x}\delta^x x S_{xy}^n\right], \tag{4.2}$$

$$E^{n+1} = E^n + \frac{\Delta t}{\rho^n}\left\{\frac{1}{x}\delta^x\left[x u^{n+1/2}(S_{xx}^n - P^{n+1/2}) + x v^{n+1/2} S_{xy}^n\right]\right\}$$
$$+ \frac{\Delta t}{\rho^n}\delta^y\left[v^{n+1/2}(S_{yy}^n - P^n) + u^{n+1/2} S_{xy}^n\right], \tag{4.3}$$

where P^n and $S_{\mu\lambda}^n$ for $(\mu = x, y;\ \lambda = x, y)$ are data-parallel arrays for pressure and stress deviator, respectively, δ^λ is the spatial derivative

$$\delta^\lambda \xi^n = \left(\xi_{1/2}^n - cshift(\xi_{1/2}^n, dim, -1)\right)/\Delta\lambda$$

with $\xi_{1/2}^n$ defined as the spatial-centered term, dim = 1,2 depending on if λ = x or y, and $\Delta\lambda$ = cshift (λ,dim,1) – λ.

Data-parallel expressions for $P_{1/2}^{n+1/2}$ are given by

$$P_{1/2}^{n+1/2} = P_{1/2}^{n} - \frac{\Delta t}{2}(\rho C_S^2)_{1/2}^{n} \frac{1}{x} \delta^x (xu)_{1/2}^{n} \tag{5}$$

for the radial direction and

$$P_{1/2}^{n+1/2} = P_{1/2}^{n} - \frac{\Delta t}{2}(\rho C_S^2)_{1/2}^{n} \delta^y (v_{1/2}^{n}) \tag{6}$$

for the axial direction. The spatial-centered pressures of Equations 5 and 6 are defined by

$$P_{1/2}^{n} = \frac{cshift(P^n,dim,1)\rho^n + P^n cshift(\rho^n,dim,1)}{\rho^n + cshift(\rho^n,dim,1)}$$

with dim depending on either the radial or axial direction. The $(\rho C_S^2)_{1/2}^{n}$ term in Equations 5 and 6, where C_S is the isentropic sound speed, is given by

$$(\rho C_S^2)_{1/2}^{n} = \min\left[(\rho C_S^2)^n,\ cshift((\rho C_S^2)^n,\ dim,\ 1)\right]$$

with $(\rho C_S^2)^n$ computed via the EOS.

Data-parallel time advanced velocities in Equation 4.3 are computed via the following expressions:

$$u_{1/2}^{n+1/2} = u_{1/2}^{n} - \left[\frac{\Delta t}{2\max(\rho^n, cshift(\rho^n,2,1))}\right](cshift(P^n,2,1) - P^n)/\Delta x,$$

$$v_{1/2}^{n+1/2} = v_{1/2}^{n} - \left[\frac{\Delta t}{2\max(\rho^n, cshift(\rho^n,1,1))}\right](cshift(P^n,1,1) - P^n)/\Delta y$$

$$- \frac{\Delta t}{4}(g + cshift(g,1,1)),$$

where $u_{1/2}^{n}$ is given by Equation 3 and $v_{1/2}^{n}$ has an analogous form.

Similar computations are carried out for the stress deviators. The numerical solution in a data-parallel format is obtained explicitly by

$$S^n_{\mu\lambda 1/2} = \Phi_{1/2} \frac{S^n_{\mu\lambda}\, cshift(\rho^n, dim, 1) + cshift(S^n_{\mu\lambda}, dim, 1)\rho^n}{\rho^n + cshift(\rho^n, dim, 1)},$$

where

$$\Phi_{1/2} = \min(VF,\ cshift(VF,\ dim,\ 1))$$

with *VF* defined as a data-parallel array describing the fractional volume of solid in a given computational cell. The stress deviators are numerically updated and are subject to the Von Mises yield criterion.

The application of the boundary conditions for the Lagrangian and advection computations is implemented through the use of data-parallel selector arrays containing values of 1.0 for selecting computational cells and values of 0.0 for deselecting cells. Selector arrays, or masked array assignments, are implemented using the WHERE statement. For example, the left reflective boundary condition for $u^n_{1/2}$ given by Equation 3 requires the left fictitious cells to hold the temporary value of $u^n_{1/2} = 0.0$. This is accomplished by multiplying the data-parallel expression for $u^n_{1/2}$ by an array containing 1.0 for all active cells and 0.0 for the left fictitious cells. Similar selector arrays are employed for implementing analogous boundary conditions.

4.3 EOS Computations. EOS calculations are, in general, good candidates for the SIMD data parallelism of the CM-2. They are characterized as being free of both interprocessor communication and grid boundary conditions. However, for multimaterial problems, EOS calculations are inherently Multiple-Instructions Multiple-Data (MIMD) type operations. The MIMD nature is due to the nonhomogeneity of the computations derived from materials with different EOS formulations (e.g., gamma law and Mie-Gruneisen) and different material parameters characterizing the same EOS (e.g., steel and rolled homogeneous armor [RHA]). Moreover, mixed material cells, which require an iterative procedure to equilibrate the

pressure for each material, induce a MIMD style of programming. Figure 4 depicts schematically the general condition for computing the EOS for a three-material simulation.

The most direct method for computing pressures employing analytic EOS expressions of the form $p = p(\rho, I)$, where I is the internal energy, is one which calculates in parallel cell pressures (partial pressures for mixed material cells) as part of a sequential loop over all materials. The calculated result is placed in a data-parallel scratch array *pp(im,:,:)*, where *im* is the material index. A logical mask is then used to segregate pure and mixed cells, with mixed cells requiring further calculations.

The problem with this method is twofold. First, there is a *nm*-factor increase in the set of required computations due to the sequential loop over the materials rather than one data-parallel SIMD computation. This can be somewhat relaxed for materials with identical EOS formulations by introducing data-parallel material property arrays for each material at each VP (or virtual grid). For virtual sets with identical materials, one array would be required. Unfortunately this determination is dynamic and not static.

The second problem deals with mixed material cells. Each mixed cell undergoes a volume iteration in an effort to compute an equilibrium pressure. During this iteration, the VPs (or virtual grids) which hold pure cells are conditionally masked such that they are inactive. As the number of iterations and mixed cells grows, the relative cycle throughput of SIMD operations decreases. Similar problems occur during the advection phase. The elimination of these problems requires asynchronous constructs and are not supported in a SIMD platform.

The SIMD methodology for computing material strength is similar to that for computing pressures. Scratch data-parallel arrays are employed to store temporary values of the shear modulus, yield strength, stress deviators, etc. for both pure and mixed material cells during volume iterations. Upon convergence, all cell values are reloaded into their respective hydrodynamic variable arrays.

4.4 Advection Computations. As mentioned above, HULL advects materials based on a first-order donor cell method. The calculation of the relative transport weights for apportioning the volume flux is carried out using the intrinsic *cshift* function for computing the fractional

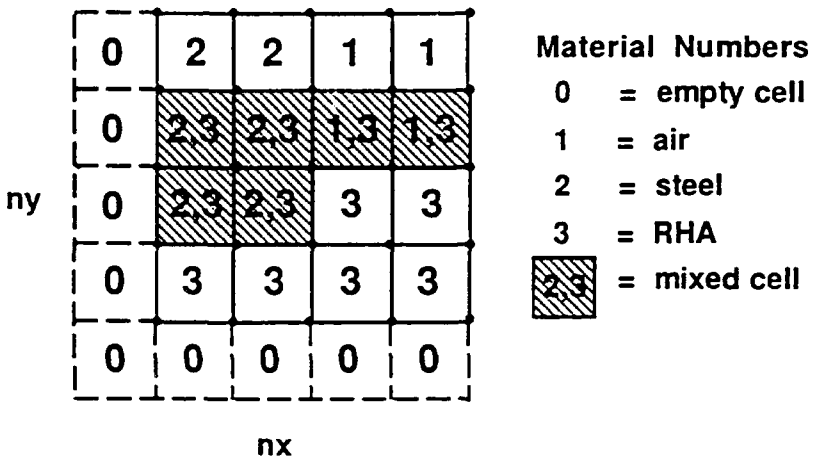

Figure 4. HULL EOS Computations.

volumes in the receiver and upstream cells. A diffusion limiter algorithm is employed in an attempt to unmix mixed material cells.

The material slices for computing transport terms are stored in a data-parallel array hs(:SERIAL, :SERIAL, :NEWS, :NEWS), where the SERIAL dimensions cover the number of materials and spatial flux directions (four in 2-D), respectively. The NEWS-ordered dimensions span the mesh space and are conformable with the advected hydrodynamic variable arrays. Volume iterations are required to reduce the flux of over-emptied materials. Convergence is checked by monitoring a data-parallel array consisting of ones and zeros.

The final remapping step is transparent in its implementation, using simple grid finite-difference quantities computed via *cshift* operations. For example, the volume of material *n*, denoted by the data-parallel array V_n, is advected to the original fixed Eulerian mesh,

$$^{e}V_n = V_n + \delta V_{n,2}(left) + \delta V_{n,3}(bottom) - \delta V_{n,4}(right) - \delta V_{n,1}(above)$$

$$= V_n + cshift(\delta V_{n,4},2,-1) + cshift(\delta V_{n,1},1,-1) - \delta V_{n,4} - \delta V_{n,1} \quad ,$$

where ${}^{e}V_n$ is the Eulerian volume and the transporting volume is

$$\delta V_{n,l} = (\Delta_{n,l} V_n)_{donor}$$

with $\Delta_{n,l}$ defined as the transport fraction for each material in particular direction l. Active cells are advected while fictitious cells along with inactive cells are masked.

5. APPLICATION AND PERFORMANCE RESULTS

The application we report here as an illustration of the computational performance is a 2-D, multimaterial computation of a steel rod impacting RHA at a striking velocity of 3 km/s (Figure 5). The computational geometry is such that the length-to-diameter ratio of the steel rod was set to 5. Material strength was implemented via an elastic-perfectly plastic formulation with the hydrodynamic behavior of materials modeled using the gamma law and Mie-Gruneisen EOS.

Calculations were performed on a 16K segment of a 32K-processor CM-2 located at the University of Minnesota. The total memory capacity is 4 Gbytes with a DataVault of 10 Gbytes. The front-end is a VAX 6420 with 64 Mbytes of memory running the ULTRIX operating system. Reprogramming of the HULL code was carried out using CM-Fortran with double-precision arithmetic implemented via the slicewise compiler.

Results for the grind times (microsec/cell/cycle) computed on the CM-2 for various mesh sizes along with the corresponding CRAY-2 single processor results are presented in Table 1. Note that all meshes were a multiple of 4, thereby optimizing the layout of data on the CM. It should be noted that meshes that are not a multiple of 4 will yield lower performance. In general, performance on the CRAY-2 is roughly constant (i.e. independent of problem size).

A comparison of the computed grind times shows the 16K-processor CM-2 performance is faster than a CRAY-2 processor. For a 512×512 mesh the CM-2 is 12 times faster. Note that the grind times for a fixed CM-2 scale inversely and nonlinearly with the virtual grid length.

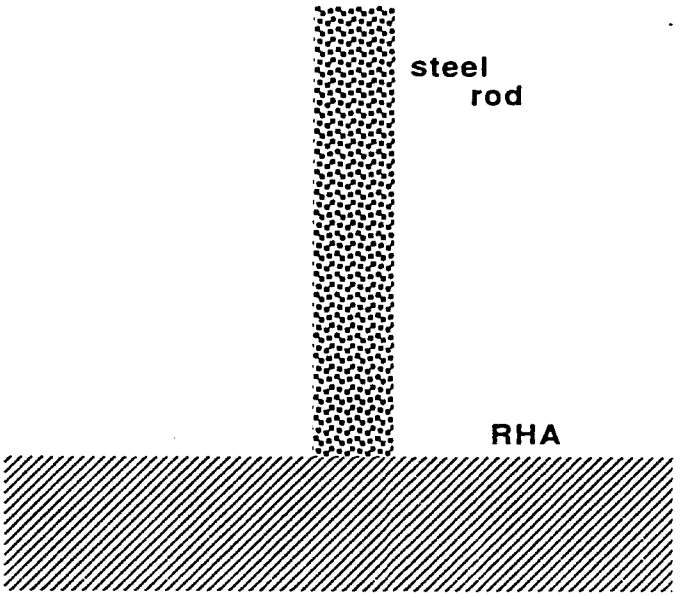

Figure 5. HULL Application on the CM-2.

Table 1. HULL Hydrocode Performance Results on the CM-2[a]

Grid Size	CM-2			CRAY-2
	VG Length[b]	Efficiency[c]	Grind Time[d]	Grind Time[d]
128 × 128	32	0.87	39	–
256 × 256	128	0.93	22	–
512 × 512	512	0.97	16	196

[a]CM-Fortran with double precision using slicewise compiler on a 16K segment.
[b]VG (virtual grid) length = number of grid points/number of FPUs.
[c]Efficiency = CM-2 execution time/CM-2 elapsed time.
[d]Grind time = μs/cell/cycle.

The observed improvement in efficiency as a function of data set size is due to the amortization of the start-up overhead over large blocks of computations and to some of the communication occurring on the same chip. The overall SIMD parallelism performance of the HULL code is limited by the EOS solution procedure employed in solving for mixed cells.

Recently developed EOS methods (McGlaun, Thompson, and Elrick 1990) appear to be more amenable to the data parallelism of the CM-2.

6. CONCLUSIONS

In this report, we have presented the initial step toward the adaptation of the HULL code for the Connection Machine. Results for a parallel implementation of a prototypical rod-plate impact calculation have been shown to be faster than the CRAY-2 results. Extrapolating the CM-2 grind times to a full 64K-processor machine suggests that this machine is capable of 50 times the performance of the CRAY-2 for executing the HULL code. However, performance is limited by the EOS calculation for the multimaterial mixed cells.

INTENTIONALLY LEFT BLANK.

7. REFERENCES

Hopson, J. W. Private communication. Los Alamos National Laboratory, 1990.

Matuska, D. A., and J. J. Osborne. "HULL Documentation: Technical Discussion Vol. I." Orlando Technology Incorporated, 1987.

McGlaun, J. M., S. L. Thompson, and M. G. Elrick. International Journal of Impact Engineering, vol. 10, pp. 351–360, 1990.

Robinson, A. C., E. Fang, D. Holdridge, J. M. McGlaun. "A Development Plan for a Massively Parallel Version of the Hydrocode CTH." Sandia National Laboratories Report SAND90-0589, 1990.

Thinking Machines Corporation, CM Fortran Reference Manual, Ver. 5.2-0.6, Cambridge, MA, 1989.

Thinking Machines Corporation, Connection Macnine Model CM-2 Technical Summary, Cambridge, MA, 1990.

Thinking Machines Corporation, CM Fortran Programming Guide, Ver. 1.0, Cambridge, MA, 1991.

INTENTIONALLY LEFT BLANK.

No. of Copies | Organization

2 Administrator
Defense Technical Info Center
ATTN: DTIC-DDA
Cameron Station
Alexandria, VA 22304-6145

1 Commander
U.S. Army Materiel Command
ATTN: AMCAM
5001 Eisenhower Ave.
Alexandria, VA 22333-0001

1 Commander
U.S. Army Laboratory Command
ATTN: AMSLC-DL
2800 Powder Mill Rd.
Adelphi, MD 20783-1145

2 Commander
U.S. Army Armament Research, Development, and Engineering Center
ATTN: SMCAR-IMI-I
Picatinny Arsenal, NJ 07806-5000

2 Commander
U.S. Army Armament Research, Development, and Engineering Center
ATTN: SMCAR-TDC
Picatinny Arsenal, NJ 07806-5000

1 Director
Benet Weapons Laboratory
U.S. Army Armament Research, Development, and Engineering Center
ATTN: SMCAR-CCB-TL
Watervliet, NY 12189-4050

(Unclass. only)1 Commander
U.S. Army Rock Island Arsenal
ATTN: SMCRI-TL/Technical Library
Rock Island, IL 61299-5000

1 Director
U.S. Army Aviation Research and Technology Activity
ATTN: SAVRT-R (Library)
M/S 219-3
Ames Research Center
Moffett Field, CA 94035-1000

1 Commander
U.S. Army Missile Command
ATTN: AMSMI-RD-CS-R (DOC)
Redstone Arsenal, AL 35898-5010

No. of Copies | Organization

1 Commander
U.S. Army Tank-Automotive Command
ATTN: ASQNC-TAC-DIT (Technical Information Center)
Warren, MI 48397-5000

1 Director
U.S. Army TRADOC Analysis Command
ATTN: ATRC-WSR
White Sands Missile Range, NM 88002-5502

1 Commandant
U.S. Army Field Artillery School
ATTN: ATSF-CSI
Ft. Sill, OK 73503-5000

2 Commandant
U.S. Army Infantry School
ATTN: ATZB-SC, System Safety
Fort Benning, GA 31903-5000

(Class. only)1 Commandant
U.S. Army Infantry School
ATTN: ATSH-CD (Security Mgr.)
Fort Benning, GA 31905-5660

(Unclass. only)1 Commandant
U.S. Army Infantry School
ATTN: ATSH-CD-CSO-OR
Fort Benning, GA 31905-5660

1 WL/MNOI
Eglin AFB, FL 32542-5000

Aberdeen Proving Ground

2 Dir, USAMSAA
ATTN: AMXSY-D
AMXSY-MP, H. Cohen

1 Cdr, USATECOM
ATTN: AMSTE-TC

3 Cdr, CRDEC, AMCCOM
ATTN: SMCCR-RSP-A
SMCCR-MU
SMCCR-MSI

1 Dir, VLAMO
ATTN: AMSLC-VL-D

10 Dir, USABRL
ATTN: SLCBR-DD-T

No. of Copies	Organization
1	Director DARPA ATTN: J. Richardson 1400 Wilson Blvd. Arlington, VA 22209-2308
2	Commander U.S. Army MICOM ATTN: AMSMI-RD-TE-F, Matt, H. Triplett Redstone Arsenal, AL 35898-5250
2	Commander U.S. Army Tank-Automotive Command ATTN: AMCPM-ABMS-SA, John Rowe AMSTA-RSS, K.D. Bishnoi Warren, MI 48397-5000
2	Commander U.S. Army Armament Research, Development, and Engineering Center ATTN: SMCAR-CCH-V, M.D. Nicolich SMCAR-FSA-E, W.P. Dunn Picatinny Arsenal, NJ 07806-5000
4	Commander U.S. Army Belvoir Research, Development, and Engineering Center ATTN: STRBE-NAE, Bryan Westlich STRBE-JMC, Terilee Hanshaw STRBE-NAN, Steven G. Bishop Josh Williams Fort Belvoir, VA 22060-5166
1	Commander U.S. Army Research Office ATTN: J. Chandra P.O. Box 12211 Research Triangle Park, NC 27709-2211
1	Commander U.S. Army Foreign Science and Technology Center ATTN: AIAST-IS 220 Seventh Street, NE Charlottesville, VA 22901-5396

No. of Copies	Organization
1	Commander Det S, USAOG USAINSCOM ATTN: IAGPC-S Fort Meade, MD 20755
1	Director U.S. Army Missile and Space Intelligence Center ATTN: AIAMS-YDL Redstone Arsenal, AL 35898-5000
1	Commander USACECOM R&D Technical Library ATTN: ASQNC-ELC-IS-L-R, Myer Center Fort Monmouth, NJ 07703-5000
5	Commander Naval Weapons Center ATTN: Code 3263, Tucker T. Yee Code 3268, Don Thompson Code 6214, W.J. McCarter Code 4057 Code 45, Tech Library China Lake, CA 93555-6001
3	Commander Naval Surface Warfare Center ATTN: Code G-22, Charles R. Garnett Code G-33, Linda F. Williams Code H-11, Mary Jane Sill Dahlgren, VA 22448-5000
2	Commander Naval Weapons Support Center ATTN: John D. Barber Sung Y. Kim Code 2024 Crane, IL 47522-5020
1	Officer-in-Charge Civil Engineering Laboratory Naval Construction Battalion Center ATTN: Code L-56, Joel Young Port Hueneme, CA 93041

No. of Copies | Organization

12 Commander
Naval Surface Warfare Center
ATTN: J. P. Matra
P. Walter
L. Mensi
K. Kiddy
F. J. Zerilli
T. Spivok
R. Phinney
C. Smith
E. Johnson
W. Bullock
C. Dickerson
10901 New Hampshire Avenue
Silver Spring, MD 20903-5000

1 Commander
Naval Surface Warfare Center
ATTN: Code 730, Library
Silver Spring, MD 20910

1 Commander
Naval EOD Technology Center
ATTN: Code 6052A, C. Cherry
Indian Head, MD 20640

1 AFATL/DLJR
ATTN: J. Foster
Eglin AFB, FL 32542

4 Air Force Armament Laboratory
ATTN: AFATL/DLJW,
W. Cook
M. Nixon
AFATL/MNW,
LT Donald Lorey
Richard D. Guba
Eglin AFB, FL 32542

1 WRDC/MTX
ATTN: Mr. Lee Kennard
Wright-Patterson AFB, OH 45433-6533

1 Central Intelligence Agency
Office of Central Reference
Dissemination Branch
Room GE-47 HQS
Washington, DC 20502

No. of Copies | Organization

5 Director
Sandia National Laboratories
ATTN: Division 1533,
P. Yarrington
M. Kipp
A. Robinson
E. Hertel
Division 1541,
J. McGlaun
P.O. Box 5800
Albuquerque, NM 87185

4 Director
Los Alamos National Laboratory
ATTN: MS P940, Robert Karpp
B216,
J. W. Hopson
D. Kothe
MS F663,
T. Adams
S. T. Bennion
MSG787, Tech Library
P.O. Box 1663
Los Alamos, NM 87545

3 Director
Lawrence Livermore National Laboratory
ATTN: L-290, John E. Reaugh
MS-35,
Michael J. Murphy
Technical Library
P.O. Box 808
Livermore, CA 94550

1 Southwest Research Institute
ATTN: C. Anderson
P.O. Drawer 28255
San Antonio, TX 78228-0255

2 Battelle
ATTN: R. Jameson
TACTEC Library, J.N. Huggins
505 King Avenue
Columbus, OH 43201-2693

No. of Copies	Organization
3	California Research and Technology, Inc. ATTN: Roland Franzen Dennis Orphal Ron E. Brown 5117 Johnson Drive Pleasanton, CA 94566
1	California Research and Technology, Inc. ATTN: Mark Majerus P.O. Box 2229 Princeton, NJ 08543
1	S-Cubed ATTN: Dr. R.T. Sedgwick P.O. Box 1620 La Jolla, CA 92083-1620
1	Orlando Technology, Inc. ATTN: Dan Matuska P.O. Box 855 Shalimar, FL 32579
3	Kaman Sciences Corporation ATTN: D. Barnette D. Elder P. Bussell P.O. Box 7463 Colorado Springs, CO 80933-7463
1	Alliant Techsystems, Inc. Defense Systems Division ATTN: G. Johnson 7225 Northland Drive Brooklyn Park, MN 55428
2	University of Minnesota Army High Performance Computing Research Center ATTN: G. Sell D. Austin 1100 Washington Ave. South Minneapolis, MN 55415

No. of
Copies Organization

1 Defense Research Establishment Suffield
ATTN: Chris Weickert
Ralston, Alberta, TOJ 2NO Ralston
CANADA

3 IABG
ATTN: H.J. Raatschen
W. Schittke
F. Scharppf
Einsteinstrasse 20
D-8012 Ottobrun B. Muenchen
GERMANY

1 Royal Armament R&D Establishment
ATTN: Ian Cullis
Fort Halstead
Sevenoaks, Kent TN14 7BJ
ENGLAND

1 Centre d'Etudes de Gramat
ATTN: SOLVE Gerald
46500 Gramat
FRANCE

1 PRB S.A.
ATTN: M. Vansnick
Avenue de Tervueren 168, Bte. 7
Brussels, B-1150
BELGIUM

INTENTIONALLY LEFT BLANK.

USER EVALUATION SHEET/CHANGE OF ADDRESS

This laboratory undertakes a continuing effort to improve the quality of the reports it publishes. Your comments/answers below will aid us in our efforts.

1. Does this report satisfy a need? (Comment on purpose, related project, or other area of interest for which the report will be used.) _____

_____

_____

2. How, specifically, is the report being used? (Information source, design data, procedure, source of ideas, etc.) _____

_____

_____

3. Has the information in this report led to any quantitative savings as far as man-hours or dollars saved, operating costs avoided, or efficiencies achieved, etc? If so, please elaborate. _____

_____

_____

4. General Comments. What do you think should be changed to improve future reports? (Indicate changes to organization, technical content, format, etc.) _____

_____

_____

BRL Report Number BRL-TR-3360 Division Symbol _____

Check here if desire to be removed from distribution list. ____

Check here for address change. ____

Current address: Organization _____
Address _____

_____

DEPARTMENT OF THE ARMY
Director
U.S. Army Ballistic Research Laboratory
ATTN: SLCBR-DD-T
Aberdeen Proving Ground, MD 21005-5066

OFFICIAL BUSINESS

BUSINESS REPLY MAIL
FIRST CLASS PERMIT No 0001, APG, MD

Postage will be paid by addressee

Director
U.S. Army Ballistic Research Laboratory
ATTN: SLCBR-DD-T
Aberdeen Proving Ground, MD 21005-5066

NO POSTAGE
NECESSARY
IF MAILED
IN THE
UNITED STATES